J Mater Sci (2008) 43:5206–5210
DOI 10.1007/s10853-008-2753-4

Initial nucleation kinetics of martensite transformation

J. R. C. Guimarães · P. R. Rios

Received: 30 March 2008 / Accepted: 23 May 2008 / Published online: 11 June 2008

Abstract The initial rate of martensite transformation in Fe–Ni and Fe–Ni–Mn is described by the product of the probability of a nucleation site existing in an austenite grain times the probability of its propagation. The former depends on driving force, the latter on defect mobility. The onset of both athermal and isothermal martensite could be modeled in a consistent way, which suggests that both modes have common fundamentals.

Introduction

It is generally accepted that the onset of martensite transformation results from the propagation of nucleation-related defects, which exist in the austenite. Such defects would have different potencies and would be scarce at the M_s temperature. However, their number increases with the driving force (the negative of the chemical free energy change) available for the reaction [1]. Martensite transformation is heterogeneous not only in the sense that nucleation takes place at preferred sites but also in the sense that it does not occur simultaneously in every austenite grains. Cech and Turnbull [2] were first to report the latter behavior, regarding martensite transformation in a Fe–30.2mass%Ni particulate of different particle sizes: '*it is the relative number of particles undergoing transformation at a given temperature that varies with particle size*'. A similar remark applies to martensite transformation in bulk polycrystalline material whether isothermally or athermally transformed. The reaction is first observed in a few clusters of partially transformed austenite grains. Following this the reaction starts elsewhere until it spreads over the whole polycrystal [3–7].

In this work, we consider the temperature dependence of the number per unit volume of nucleation-related defects characteristic of particulate Fe–30.2mass%Ni athermal transformation, as basis to model the initial reaction rate of isothermally transformed bulk Fe–23.2mass%Ni–2.8 mass%Mn. In both alloys, plate martensite is formed at sub-zero temperatures.

Model development

Cohen and Olson [1] reviewed the data from Cech and Turnbull [2] and concluded that the probability that at least one nucleation site exists in a particle of mean volume q is exponentially related to the number per unit volume of material of sites for martensite nucleation, n_{v}^{T}, available to propagate down to temperature T

$$P_{\mathrm{q}}(T) = 1 - \exp\left(-qn_{\mathrm{v}}^{T}\right) \tag{1}$$

where a T superscript means 'at temperature T'.

Moreover, for a large ensemble of particles, $P_{\mathrm{q}}(T)$ can be equated to the volume fraction of material in partially transformed particles, $V_{\mathrm{v}}^{\mathrm{g}}$, the parameter used to describe the extent of the spread of martensite transformation over the austenite grains in a bulk polycrystalline material, thus, $P_{\mathrm{q}}(T) = V_{\mathrm{v}}^{\mathrm{g}}$. This is justified by the fact that one nucleation event is enough to partially transform a particle; therefore, in the absence of particle–particle interaction, $V_{\mathrm{v}}^{\mathrm{g}}$ is directly

J. R. C. Guimarães · P. R. Rios (✉)
Universidade Federal Fluminense, Escola de Engenharia Industrial Metalúrgica de Volta Redonda, Av. dos Trabalhadores, 420, Volta Redonda, RJ 27255-125, Brazil
e-mail: prrios@metal.eeimvr.uff.br

J. R. C. Guimarães
Mal. Moura 338H/22C, Sao Paulo, SP 05641-000, Brazil

related to n_v^T. By considering V_v^g to investigate the initial nucleation rate we can avoid the complication of autocatalysis.

The initial rate of an isothermal martensite reaction $dN_{v,0.002}/dt$, is commonly determined at 0.002 volume fraction transformed

$$\frac{dN_{v,0.002}}{dt} = n_v^i v \exp\left(-\frac{W_a^*}{kT}\right), \quad (2)$$

where v is the lattice frequency, n_v^i the initial number of nucleation sites per unit volume, and W_a^* is the activation energy for martensite nucleation, k is the Boltzmann constant and T is the absolute temperature [8, 9].

We propose here that the *initial* reaction rate at temperature T, I_v, is given by the product of P_q^T the probability of nucleation site availability times P_P^T,the probability that an existing nucleation site may propagate

$$\frac{dN_v}{dt} = I_v = \frac{v}{q} P_q^T P_P^T. \quad (3)$$

By similarity with Eq. 2 we consider P_P^T to be thermally activated, thus, $P_P^T = \exp\left(-\frac{E_P}{kT}\right)$,where E_P is the activation energy for propagation. Inserting P_q^T and P_q^T into Eq. 3 gives the initial rate of martensite reaction per unit grain volume

$$I_v = \frac{v}{q}\left[1 - \exp\left(-qn_v^T\right)\right] \exp\left(-\frac{E_P}{kT}\right). \quad (4)$$

Athermal martensite transformation in particulated Fe–30.2%massNi

To obtain values of n_v^T, we pursued Cohen and Olson [1] and recovered data from Cech and Turnbull [2] by scanning and digitizing their graphs. Non-conspicuous data points were dismissed. The compiled data, typical of athermal transformation in particulate Fe–30.2%massNi, have been consolidated by reiteration to average out small variations. The grain volume was calculated from the particle diameter, D, by $q = \pi D^3/6$. Recalling that $P_q(T) = V_v^g$, Eq. 1 can be rewritten as

$$\ln\left(\frac{1}{1 - P_q^T}\right) = \ln\left(\frac{1}{1 - V_v^g}\right) = qn_v^T. \quad (5)$$

Figure 1 shows $\ln\left(\frac{1}{1-V_v^g}\right)$ plotted against q at the indicated temperatures. Linear regression of the data exhibits high correlation coefficients, R, as shown in Table 1. Thus n_v^T should not depend on the particle size, and its value can be calculated from the slope of the straight lines fitted to the data. Table 1 depicts these values of n_v^T which increase with increasing the reaction driving force. Athermal martensite transformation starts when the

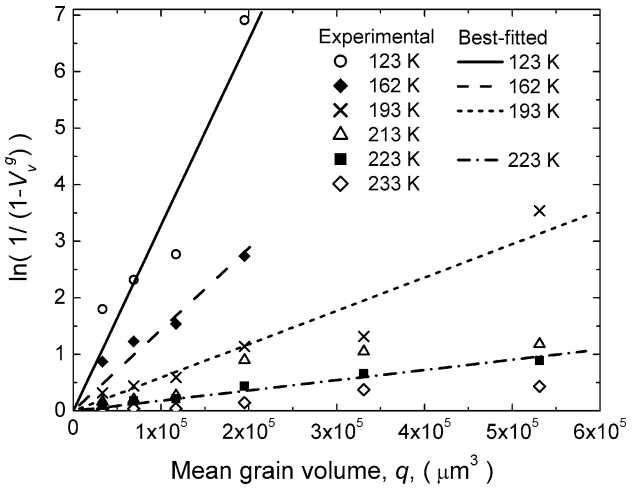

Fig. 1 Volume fraction of partially transformed particles shown as a function of particle volume and transformation temperature, data from Cech and Turnbull [2]. Some best-fit straight lines are not shown to avoid overloading the figure

Table 1 Regression results from Fig. 1 and values of n_v^T

Temperature (K)	ΔG (J event^{-1}) (10^{-21})	n_v^T (mm^{-3})	R
233	1.990	$8.73 \cdot 10^2$	0.96
223	2.074	$1.81 \cdot 10^3$	0.98
213	2.157	$2.67 \cdot 10^3$	0.89
193	2.317	$5.90 \cdot 10^3$	0.96
162	2.552	$1.44 \cdot 10^4$	0.94
123	2.820	$2.78 \cdot 10^4$	0.93

driving force, ΔG reaches a certain threshold indicated by the M_s temperature and, frequently, by a burst. As a working hypothesis n_v^T is assumed to increase with the excess of driving force with respect to some threshold driving force, ΔG_0,

$$n_v^T \propto \Delta G - \Delta G_0, \quad (6)$$

where ΔG is the driving force available for the transformation. This proportionality may be expressed as equality by introducing a pre-factor n_v^0 and dividing the excess driving force by kT

$$n_v^T = n_v^0\left(\frac{\Delta G - \Delta G_0}{kT}\right), \quad (7)$$

where n_v^0 stands for the value of n_v^T when $\Delta G - \Delta G_0 = kT$. To check the concept, the data in Table 1 were plotted as shown in Fig. 2. The values of ΔG were calculated after Kaufman and Cohen [10].

A parametric least-square procedure was used to obtain the values of ΔG_0 and of n_v^0 that allow best fit of the data with Eq. 7. The values of these parameters are given in Table 2. Inspection of Fig. 2 discloses a high correlation

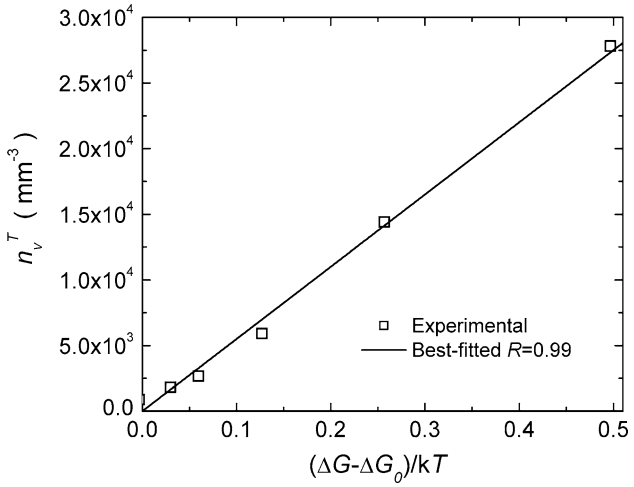

Fig. 2 Values of n_v^T graphed as per Eq. 7. The slope of this plot is equal to n_v^0

Table 2 Regression results from particulate data plotted in Fig. 2

n_v^0 (mm^{-3})	$5.5 \cdot 10^4$
ΔG_0(J event$^{-1)}$	$2.0 \cdot 10^{-21}$
R	0.99

fitting. Noteworthy, ΔG_0 is not far from ΔG at the highest transformation temperature. As one might expect, the value of n_v^0 obtained here, $5.54 \cdot 10^4$ mm^{-3}, is in agreement with the value of n_v^i, 10^4 mm^{-3}, normally admitted.

Eq. 7 may be substituted for n_v^T in Eq. 4

$$I_v = \frac{v}{q}\left[1 - \exp\left(-qn_v^0\left(\frac{\Delta G - \Delta G_0}{kT}\right)\right)\right]\exp\left(-\frac{E_P}{kT}\right). \tag{8}$$

At higher temperatures, when the reaction is first detected, $(\Delta G - \Delta G_0)/kT$ is small. Therefore, the bracketed term in Eq. 8 simplifies ($x \cong 1-e^{-x}$) yielding

$$I_v = vn_v^0\left(\frac{\Delta G - \Delta G_0}{kT}\right)\exp\left(-\frac{E_P}{kT}\right). \tag{9}$$

Moreover, if E_P/kT is small (e.g. athermal mode of transformation) the initial reaction rate will be much faster and I_v becomes

$$I_v = vn_v^0\left(\frac{\Delta G - \Delta G_v}{kT}\right). \tag{10}$$

In fact, it has been already suggested that the martensite burst is a very fast isothermal reaction [11]. Notice that, since $I_v = vn_v$, Eq. 7 is recovered. Returning to Eq. 8, at lower temperatures, below the elbow of the C-curve, kT and $\frac{\Delta G - \Delta G_0}{kT}$ become large so that I_v approaches

$$I_v = \frac{v}{q}\exp\left(-\frac{E_P}{kT}\right). \tag{11}$$

Thus, a simple Arrhenius plot allows determining E_P. Remarkably, Eqs. 9–11 inferred from the analysis of *athermal* martensite transformation in particulate Fe–30.2mass%Ni, meet some results derived from application of classical reaction rate theory to isothermal martensite by Borgenstam and Hillert [12]. Nonetheless they were obtained upon distinct hypothesis.

Analysis of isothermal martensite transformation in Fe–23.2mass%Ni–2.8mass%Mn

In the sequence, the C-curve of isothermal martensite transformation in Fe–23.2mass%Ni–2.8mass%Mn will be analyzed based upon Eq. 9. The data used for that purpose were originally determined as described and tabulated by Ghosh and Raghavan [9] . The authors extensively described and discussed their experimental methods and conditions and that will not be repeated here for brevity. We selected their tabulated results for 0% (annealed), 1%, and 2% plastic deformed material, and elastic stressed (60.8 MPa) comprising a broad range of temperature and conditions. A plot of the transformation temperatures against nucleation rate at $V_v = 0.002$, $dN_{v,0.002}/dt$, yields C-curves of the start of isothermal martensite transformation. A plot of C-curves from their data is shown in Fig. 3. Substituting $dN_{v,0.002}/dt$ for I_v in Eq. 9 yields

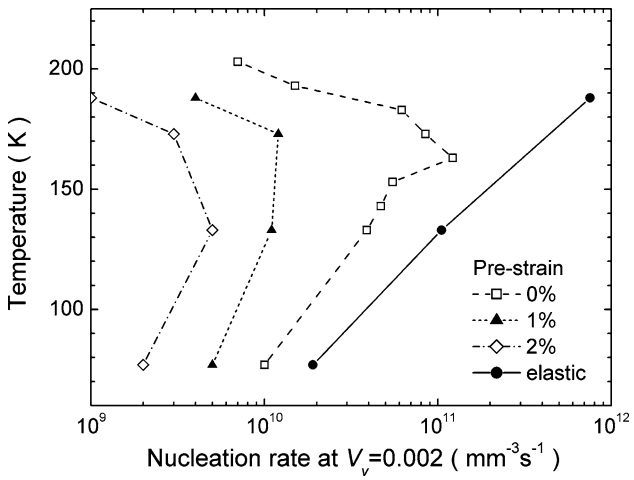

Fig. 3 Transformation temperature plotted against initial nucleation rate of isothermal martensite, $dN_{v,0.002}/dt$, in Fe–23.2mass%Ni–2.8mass%Mn under elastic load and after different amounts of plastic deformation, data from Ghosh and Raghavan [9]. C-curves are apparent, except for the elastic deformation

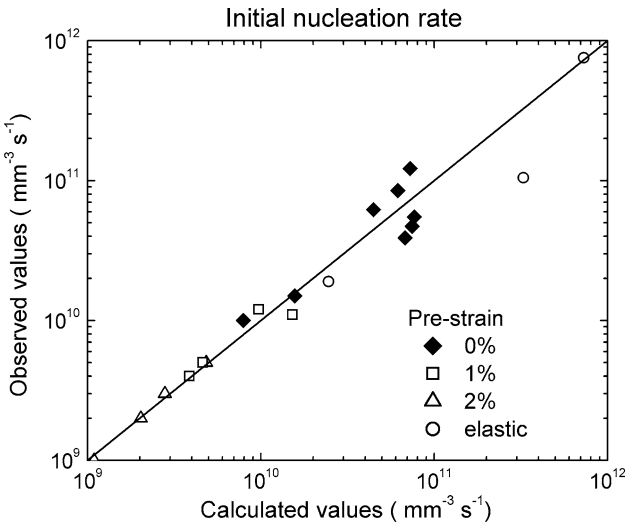

Fig. 4 Initial nucleation rate of isothermal martensite, $dN_{v,0.002}/dt$, in Fe–23.2%massNi–2.8%massMn. Experimental data from Ghosh and Raghavan [9] plotted against the values calculated by Eq. 12. The solid line of slope equal to one is drawn as a reference line

Table 3 Regression parameters obtained by best-fitting Eq. 12 to Ghosh and Raghavan's [9] data for isothermal martensitic transformation in a Fe–23.2mass%Ni–2.8mass%Mn under elastic load and after different amounts of plastic deformation

Pre-strain (%)	0	1	2	Elastic
n_v^0 (mm^{-3})	$3.8 \cdot 10^{-09}$	$2.4 \cdot 10^{-10}$	$5.0 \cdot 10^{-11}$	$3.8 \cdot 10^{-09}$
ΔG (J event^{-1})	$2.9 \cdot 10^{-21}$	$2.9 \cdot 10^{-21}$	$2.9 \cdot 10^{-21}$	$1.8 \cdot 10^{-21}$
E_P (J event^{-1})	$7.5 \cdot 10^{-21}$	$5.1 \cdot 10^{-21}$	$4.3 \cdot 10^{-21}$	$8.0 \cdot 10^{-21}$
R	0.93	0.98	0.99	0.96

A plot of their data is shown in Fig. 3

$$\frac{dN_{v,0.002}}{dt} = vn_v^0\left(\frac{\Delta G - \Delta G_0}{kT}\right)\exp\left(-\frac{E_P}{kT}\right). \quad (12)$$

The least-squares procedure used to analyze the particulate data, Fig. 1, was applied also to the data from Ghosh and Raghavan (see Fig. 3.). The experimental versus calculated values of $dN_{v,0.002}/dt$ are shown in Fig. 4. The parameters obtained are given in Table 3.

Temperature independent E_P values were obtained in all cases. Actually, the values of E_P ($4.3 - 8 \cdot 10^{-21}$ J event^{-1}) are similar in magnitude to the activation energy ($\sim 4 \cdot 10^{-21}$ J event^{-1}) for the 'growth of a martensite embryo' obtained by Kurdjumov and Maximova [12–14]. Therefore, propagation as used here and 'embryo growth' are equivalent expressions. However, these E_P values are one order of magnitude less than the values of W_a^* ($4.07 - 10.8 \cdot 10^{-20}$ J event^{-1}) reported by Ghosh and Raghavan [9]. This can be ascribed to the fact that to calculate W_a^* in Eq. 2 a temperature independent number of initially available nucleation sites, n_v^i, was assumed.

In the framework now described, bearing the behavior of Fe–30.2mass%Ni particulate, the number of sites initially available to propagate the reaction, n_v^T, is typical of the reaction temperature.

The value of ΔG_0 in Table 3 is about the same as the driving force at the highest reaction temperature and that was not affected by plastic deformation. However, elastic loading increased ΔG_0, as expected, since it is known that the austenite stability is decreased by an external (elastic) stress [15]. The hindering effect of small plastic strain on isothermal martensite, also observed in athermal martensite [16], has been previously reported [9].

Concerning n_v^0, it is not clear at present why so widely different values are obtained for the athermal and the isothermal modes of martensite transformation. Nonetheless, the existence of common fundamentals between athermal and isothermal modes of martensite transformation was pointed out by Kakeshita et al. [17] supported by experimental results pertaining to martensite transformation under magnetic field and hydrostatic pressure.

Summary and conclusions

In summary, by considering the temperature dependence of the density of preferred nucleation sites for the initial nucleation of martensite n_v^T we could describe the onset of martensite transformation either in athermal or isothermal mode in a consistent way. The importance of thermal activation in martensite transformation becomes prominent at low temperatures (high driving force) under ordinary conditions. The magnitude of the apparent activation energy obtained supports the concept that propagation depends upon defect mobility [12].

Acknowledgements One of the authors (P. R. RIOS) is grateful to Conselho Nacional de Desenvolvimento Científico e Tecnológico, CNPq, and to Fundação de Amparo à Pesquisa do Estado do Rio de Janeiro, FAPERJ, for financial support. Thanks are due to Chris Hoffman (RMC Inc.) for his valuable assistance with the bibliography.

References

1. Cohen M, Olson GB (1976) Suppl Trans JIM 17:93
2. Cech RE, Turnbull D (1956) Trans AIME 206:124
3. Brook R, Entwisle AR (1965) J Iron Steel Inst 203:905
4. Raghavan V (1969) Acta Metall 17:1299. doi:10.1016/0001-6160(69)90145-X
5. Guimarães JRC, Gomes JC (1978) Acta Metall 26:1591. doi:10.1016/0001-6160(78)90068-8
6. Ghosh G (1988) Mater Sci Eng A 101:213. doi:10.1016/0025-5416(88)90809-9
7. Rios PR, Guimarães JRC (2007) Scr Mater 57:1105. doi:10.1016/j.scriptamat.2007.08.019

8. Shih CH, Averbach BL, Cohen M (1955) Trans AIME 203:183
9. Ghosh G, Raghavan V (1986) Mater Sci Eng A 80:65. doi:10.1016/0025-5416(86)90303-4
10. Kaufman L, Cohen M (1958) Prog Met Phys 7:165. doi:10.1016/0502-8205(58)90005-4
11. Entwisle AR, Feeney JA (1969) In: Nicholson RB (ed) The Mechanism of phase transformations in crystalline solids, Institute of Metals, London, pp 156–161
12. Borgenstam A, Hillert M (1997) Acta Mater 45:651. doi:10.1016/S1359-6454(96)00186-3
13. Kurdjumov GV, Maximova OP (1948) Dokl Akad Nauk SSSR 61:83
14. Kurdjumov GV, Maximova OP (1950) Dokl Akad Nauk SSSR 73:95
15. Patel JR, Cohen M (1953) Acta Metall 1:531. doi:10.1016/0001-6160(53)90083-2
16. Gooch TG, West DRF (1967) J Iron Steel Inst 205:555
17. Kakeshita T, Katsuyama J, Fukuda T, Saburi T (2001) Mater Sci Eng A 312:219. doi:10.1016/S0921-5093(00)01878-5